Anisotropy of 2H-$NbSe_2$ in the superconducting and charge density wave states

Chi Zhang(张驰)[1,2,4,5], Shan Qiao(乔山)[1,4,5], Hong Xiao(肖宏)[3], and Tao Hu(胡涛)[2,†]

[1] *State Key Laboratory of Functional Materials for Informatics, Shanghai Institute of Microsystem and Information Technology, Chinese Academy of Sciences, Shanghai* 200050, *China*

[2] *Beijing Academy of Quantum Information Sciences, Beijing* 100193, *China*

[3] *Center for High Pressure Science and Technology Advanced Research, Beijing* 100094, *China*

[4] *CAS Center for Excellence in Superconducting Electronics (CENSE), Shanghai* 200050, *China*

[5] *University of Chinese Academy of Sciences, Beijing* 100049, *China*

(Received 21 April 2022; revised manuscript received 10 June 2022; accepted manuscript online 22 July 2022)

Anisotropy is an important feature of layered materials, and a large anisotropy is usually related to the two-dimensional characteristics. We investigated the anisotropy of the layered transition metal dicalcogenide 2H-$NbSe_2$ in the superconducting and charge density wave (CDW) states using magnetotransport measurements. In the superconducting state, the normalized $H_{c2}^{||c}/H_p$ is independent of the thickness of 2H-$NbSe_2$, while $H_{c2}^{||ab}/H_p$ increases significantly with decreasing thickness, where H_p is the Pauli limiting magnetic field and $H_{c2}^{||c}$ and $H_{c2}^{||ab}$ are the upper critical fields in the c and ab directions, respectively. It is found that the superconducting anisotropy parameter $\gamma_{H_{c2}} = H_{c2}^{||ab}/H_{c2}^{||c}$ increases with reduction in the thickness of 2H-$NbSe_2$. In the CDW state, the angular (θ) dependence of magnetoresistance, $R(H,\theta)$ scales with $H(\cos^2\theta + \gamma_{CDW}^{-2}\sin^2\theta)^{1/2}$, which decreases with increasing temperature and disappears at about 40 K. It is found that the CDW anisotropy parameter γ_{CDW} is much larger than the effective mass anisotropy but does not change a lot for ultrathin and bulk samples. Our results suggest the existence of three-dimensional superconductivity and quasi-two dimensional CDWs in bulk 2H-$NbSe_2$.

Keywords: anisotropy, superconductivity, charge density wave, transition metal dicalcogenides

PACS: 74.70.–b, 74.78.–w, 74.25.F–

DOI: 10.1088/1674-1056/ac8343

1. Introduction

The presence of a charge density wave (CDW) in a superconductor is of special interest, since CDWs exhibit a periodic modulation of electronic charge density[1] while superconductivity usually has a homogeneous charge distribution. Competition in electronic charge density usually results in unconventional superconductivity, such as in cuprates, iron pnictides and heavy fermion superconductors.[2–8] Interestingly, recent experiments have shown that CDWs coexist with superconductivity in 2H-$NbSe_2$ even down to the monolayer limit.[9,10] 2H-$NbSe_2$ belongs to the family of transition metal dicalcogenides (TMDCs). For bulk 2H-$NbSe_2$, the superconducting transition temperature T_c is 7.2 K, which is the highest known among TMDCs, and incommensurate CDW order is present at $T_{CDW} = 33$ K.[11–14] The superconductivity is strongly correlated to the CDW order in bulk 2H-$NbSe_2$.[15]

Compared with bulk 2H-$NbSe_2$, the superconductivity is substantially modified in ultrathin samples.[16,17] The two-gap superconductivity[18] in the bulk 2H-$NbSe_2$ structure changes to anisotropic single-gap superconductivity in the thin-film sample.[19] Furthermore, it was found that T_c of 2H-$NbSe_2$ decreases with decreasing sample thickness.[19–21] Such a suppression of T_c is attributed to the superconductor–vacuum interface in ultrathin 2H-$NbSe_2$ which suppresses the Cooper pair density.[19] Despite the suppression of T_c, the in-plane upper critical field arrives at six times the Pauli paramagnetic limit in monolayer 2H-$NbSe_2$.[22] The extremely large in-plane upper critical field is attributed to the strong intrinsic spin–orbit interactions, which lock the electron spin in the out-of-plane direction in ultrathin 2H-$NbSe_2$ but can be destroyed by the interlayer coupling in thick samples.[22] On the other hand, the properties of the CDW are also modified in ultrathin 2H-$NbSe_2$.[9,10] T_{CDW} in monolayer 2H-$NbSe_2$ is 145 K,[9] much higher than the 33 K in the bulk sample. Scanning tunnelling spectroscopy measurements have revealed that the CDW gap in monolayer 2H-$NbSe_2$ is 4 meV,[10] much less than the gap value of 12 meV–35 meV in the bulk sample.[23–25]

Anisotropy is another important feature of ultrathin 2H-$NbSe_2$. As a layered TMDC, ultrathin 2H-$NbSe_2$ is supposed to have a larger anisotropy than bulk samples owing to the interlayer coupling of CDWs.[26–28] The formation of a CDW has a significant influence on the electric transport properties.[29–33] For TMDC materials, the magnetoresistance (MR) caused by a CDW usually exhibits a large and linear magnetic field dependence behavior.[34,35] Such CDW

†Corresponding author. E-mail: hutao@baqis.ac.cn

© 2023 Chinese Physical Society and IOP Publishing Ltd

MR was found to be anisotropic and sensitive to the relative orientation between the magnetic field and the CDW chain axis.[36–38] Thus the electronic transport anisotropy reveals an intrinsic characteristic of CDWs in 2H-$NbSe_2$.

In this paper, we investigate the electronic transport anisotropy of 2H-$NbSe_2$. An ultrathin 2H-$NbSe_2$ device (5–10 layers) is fabricated by the mechanical exfoliation method and electrode transfer technique. In the superconducting state, the anisotropy parameter ($\gamma_{H_{c2}}$) is determined by the ratio of the upper critical fields at in- and out-of-plane directions. The anisotropy of superconductivity increases significantly with decrease in the sample thickness. In the normal state, the anisotropy parameter (γ_{CDW}) is obtained according to the angular-dependent magnetoresistance (ADMR). The ADMR obeys the scaling behavior of ADMR $= f[H(\cos^2\theta + \gamma_{CDW}^{-2}\sin^2\theta)^{1/2}]$ at 8 K and disappears at above the CDW temperature (T_{CDW}). In contrast to γ_{CDW}, the value of $\gamma_{H_{c2}}$ increases significantly as the thickness of 2H-$NbSe_2$ decreases. Our results suggest three-dimensional superconductivity and a quasi-two dimensional CDW in 2H-$NbSe_2$.

2. Experiment

The ultrathin 2H-$NbSe_2$ device is fabricated based on our previous technique.[39] The fabrication process comprises the following three steps. (i) Fabrication of Au electrodes coated with polyvinyl alcohol (PVA) film. The Au electrode patterns are fabricated on a silicon wafer by ultraviolet lithography and metal thermal evaporation technology. Then a home-made 8% PVA solution is dripped onto the Au electrodes prefabricated on the silicon wafer. After 5 h in a drying oven, the Au electrodes coated with the dry PVA film are taken out of the silicon wafer and are ready for electric feedthrough and protective use. (ii) Fabrication of ultrathin samples. Ultrathin samples are obtained based on the traditional mechanical exfoliation method for graphene. Bulk single crystal 2H-$NbSe_2$ from a commercial supplier (HQ Graphene) is exfoliated into layers using Scotch tape in an ambient environment. Then the 2H-$NbSe_2$ flakes are pressed on the Si/SiO_2 substrate. Thin flakes are distinguished under an optical microscope by their color and removed from the Si/SiO_2 substrate with a PVA film. (iii) Encapsulation processes. A selected flake of 2H-$NbSe_2$ in a PVA film is accurately transferred onto the top of the prefabricated Au electrodes in the PVA film using a sample transfer stage under the microscope. Thus the encapsulation and electric feedthrough processes are done simultaneously. Since the Au electrodes are prefabricated, the dry-transfer and the encapsulation processes can be done in 5 min to avoid damage to the 2H-$NbSe_2$ sample.

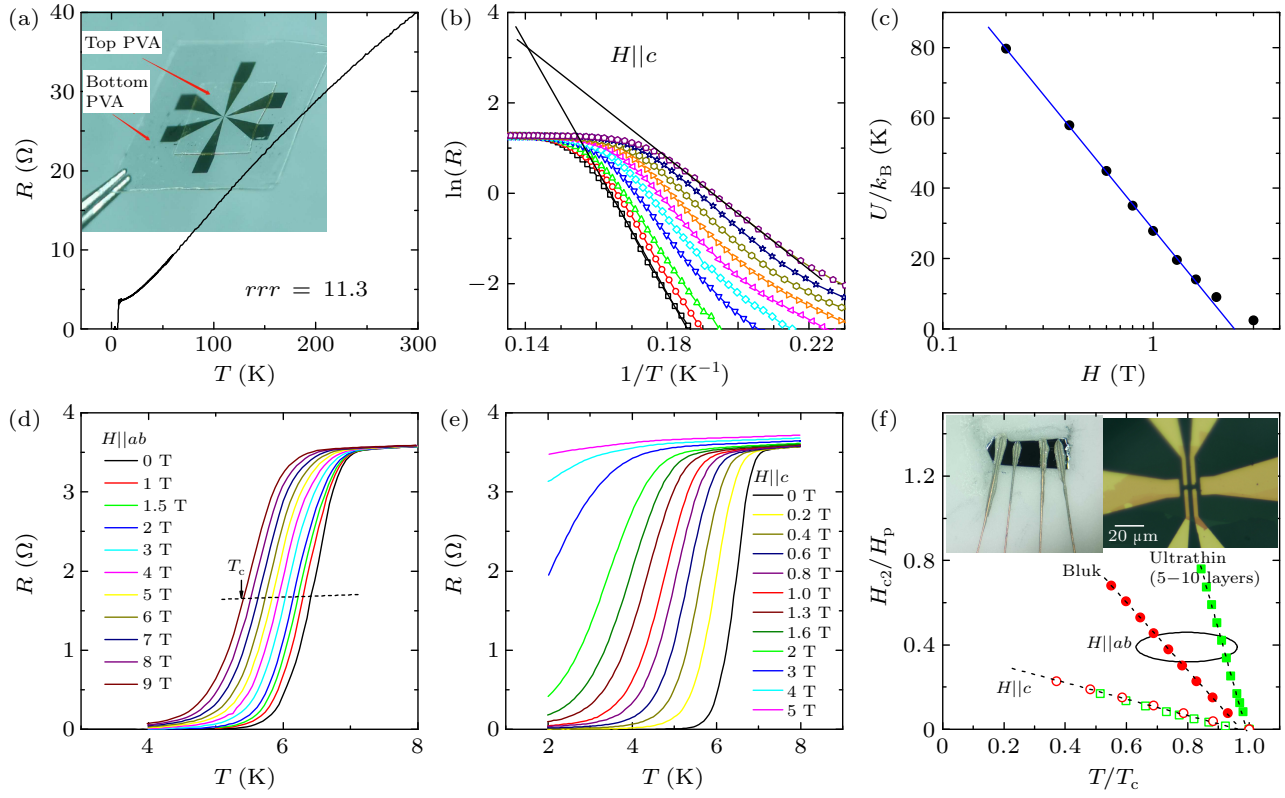


Fig. 1. The superconducting properties of an ultrathin 2H-$NbSe_2$ sample. (a) The resistance R versus temperature T. Inset: optical image of the ultrathin 2H-$NbSe_2$ device. (b) Arrhenius plots for ultrathin 2H-$NbSe_2$ at $H||c$. (c) The H dependence of activation energy U. The $R(T)$ curves under the applied H for $H||ab$ (d) and $H||c$ (e). (f) The normalized upper critical field H_{c2}/H_p versus the reduced temperature T/T_c for the bulk and ultrathin samples. The inset of Fig. 1(f) shows images of the bulk and ultrathin (5–10 layers) 2H-$NbSe_2$.

A panorama of our device is shown in the inset of Fig. 1(a). The ultrathin 2H-$NbSe_2$ sample is encapsulated by the top and bottom PVA layers. The inset of Fig. 1(f) shows an enlarged image of our device, with the 2H-$NbSe_2$ sample and the Au electrodes. The thickness of the ultrathin samples exfoliated on the Si/SiO_2 substrate can be determined by optical contrast and confirmed by atomic force microscopy (AFM). Different colors correspond to different numbers of 2H-$NbSe_2$ layers. Nevertheless, when the sample is in a flexible substrate it is hard to determine the thickness of the sample by optical contrast and AFM. Thus we only estimate the thickness of our ultrathin sample based on optical contrast before it is taken out of the Si/SiO_2 substrate. The estimated thickness of the ultrathin sample in this work is about 5–10 layers, which is still much thinner than the bulk sample.

3. Discussion

Figure 1(a) shows the resistance (R) as a function of temperature (T) for an ultrathin 2H-$NbSe_2$ sample. The residual resistance ratio $rrr = R(300\ \mathrm{K})/R(8\ \mathrm{K})$ is about 11.3. It is found that R decreases as T decreases and transits into the superconducting state at the critical temperature $T_c \approx 7$ K, which is consistent with previous reports for 2H-$NbSe_2$ single crystals.[40] The thickness of the ultrathin sample can be estimated according to the thermally activated flux-flow behavior of 2H-$NbSe_2$.[41] We therefore show in Fig. 1(b) the Arrhenius plots for ultrathin 2H-$NbSe_2$ with an out-of plane magnetic field 1 T $\leq H \leq$ 9 T. The flux-flow resistivity in the thermal activation regime can be expressed in the formula $\rho(H,T) = \rho_0 \exp(-U/k_B T)$, where U is the thermal activation energy, ρ_0 is a factor independent of the magnetic field and k_B is the Boltzmann constant. The obtained U at different magnetic fields are shown in Fig. 1(c). It is found that the thermal activation energy U can be expressed by the relationship $U = U_0 \log(H/H_0)$ with $U_0 = 73.6k_B$ in agreement with the long-range vortex–vortex interactions in a two-dimensional system.[42,43] Interestingly, the parameter of U_0 in ultrathin 2H-$NbSe_2$ was previously found to be proportional to the layer number, with $13.44k_B$ per layer.[41] Thus the thickness of our ultrathin 2H-$NbSe_2$ is more than five layers, which is consistent with the results estimated from the optical contrast.

Figures 1(d) and 1(e) show the $R(T)$ curves under the applied magnetic fields (H) along with the out-of-plane and in-plane directions respectively. We define $T_c(H)$ as the superconducting transition temperature for various H, at which the R drops to 50% of the normal state's resistance. The obtained $T_c(H)$s, or the upper critical fields $H_{c2}(T)$s, are normalized by the Pauli paramagnetic limit $H_p(T) \sim 1.84T_c$. The $H_{c2}(T)/H_p$s for the bulk and ultrathin 2H-$NbSe_2$ are summarized in Fig. 1(f). Inset of Fig. 1(f) shows the images of the bulk and ultrathin 2H-$NbSe_2$.

In Fig. 1(f), we show $H_{c2}^{||c}/H_p$ (hollow symbols) and $H_{c2}^{||ab}/H_p$ (solid symbols) as a function of the reduced temperature T/T_{c0}, where $H_{c2}^{||c}$ and $H_{c2}^{||ab}$ are the upper critical fields at c and ab crystalline directions, respectively. It is found that $H_{c2}^{||c}/H_p$ is independent of the thickness, while $H_{c2}^{||ab}/H_p$ increases significantly as the thickness of 2H-$NbSe_2$ decreases. The thickness independence of $H_{c2}^{||c}$ was previously observed and attributed to the orbital pair-breaking effect on an out-of plane critical field.[22] while $H_{c2}^{||ab}$ was interpreted in terms of the strong intrinsic spin–orbit interactions effect present in a single layer, which can lock the electronic spin in the out-of-plane direction and consequently lead to the remarkably large $H_{c2}^{||ab}$ in ultrathin 2H-$NbSe_2$.[22] Furthermore, interlayer coupling favors electron hopping between layers, which therefore enhances the orbital depairing effect and suppresses the in-plane upper critical field in the bulk sample.

It is worth noticing that $H_{c2}^{||c}$ and $H_{c2}^{||ab}$ both roughly exhibit a linear-dependent behavior of T in the investigated T range. Thus we can roughly estimate the superconducting anisotropy $\gamma_{H_{c2}} = H_{c2}^{||ab}/H_{c2}^{||c}$ for these samples. It is found that $\gamma_{H_{c2}}$ is 17.7 and 4.65 for the ultrathin and the bulk samples, respectively. Since the thickness of the ultrathin sample is beyond the atomic limit (≤ 4 layers), whether the sample is odd- or even-layered should not play a role in the anisotropy physics mechanism. Thus the significant suppression of $\gamma_{H_{c2}}$ indeed reflects a strong interlayer coupling effect on superconductivity, which causes three-dimensional superconductivity in the bulk 2H-$NbSe_2$.

It is also interesting to know the dimensional characteristics of the CDW in 2H-$NbSe_2$. We therefore investigate the MR of 2H-$NbSe_2$ in the normal state, for example $T \geq 8$ K. Figure 2(a) shows the temperature (T) dependence of resistance R (left axis) measured at magnetic fields $H = 0$ and 9 T with H along the c-axis of the crystal. The corresponding MR $(R(9\ \mathrm{T})/R(0\ \mathrm{T}) - 1)$ is plotted in Fig. 2(a) on the right axis. It is found that the MR decreases with increasing the T and becomes negligible above 40 K, which is around $T_{CDW} = 33$ K, the CDW transition temperature of bulk 2H-$NbSe_2$.[11–14] T_{CDW} was previously determined by a dip in the derivative of resistance with respect to temperature $dR(T)/dT$.[9] However, here we cannot determine the exact value of T_{CDW} in ultrathin 2H-$NbSe_2$ since the $dR(T)/dT$ feature becomes negligible in the ultrathin case. An option to determine T_{CDW} in ultrathin 2H-$NbSe_2$ is terahertz Raman spectroscopy,[15] which we leave for future work. Nevertheless, since the ultrathin sample comprises around 5–10 layers, as discussed above, T_{CDW} is about 80 K–50 K according to a previous report,[9] which is not far from 40 K.

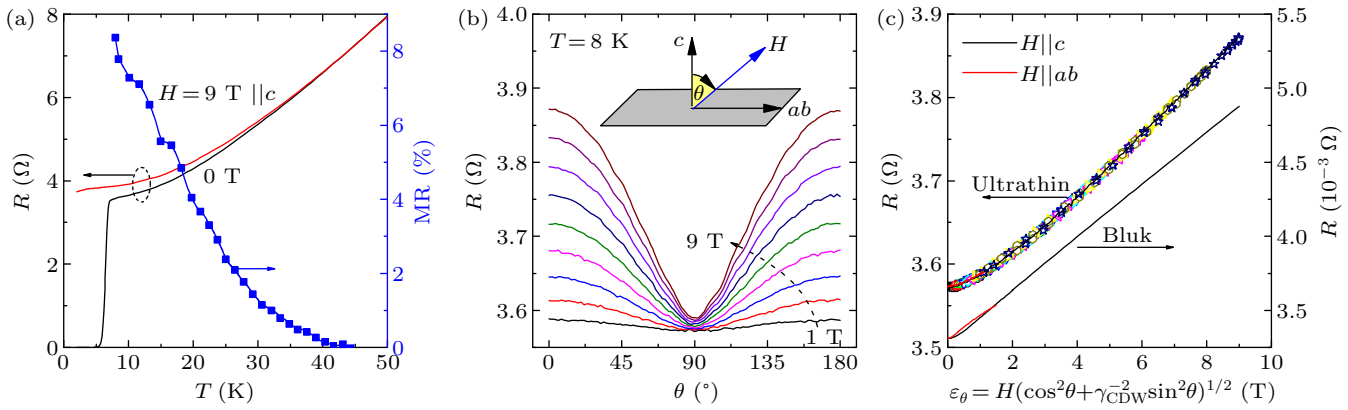


Fig. 2. The magnetoresistance (MR) of ultrathin 2H-$NbSe_2$. (a) The temperature (T) dependence of resistance (R) at $H = 0$ and 9 T (left axis), and MR equal to $R(9\ \mathrm{T})/R(0\ \mathrm{T}) - 1$ (right axis) with H applied in the c direction. (b) R versus θ measured at $T = 8$ K and $1\ \mathrm{T} \le H \le 9\ \mathrm{T}$. θ is the angle between H and the c crystalline direction as shown in the inset of panel (b). (c) R versus $H(\cos^2\theta + \gamma_{\mathrm{CDW}}^{-2}\sin^2\theta)^{1/2}$ at $T = 8$ K for the ultrathin and bulk samples. The symbols are taken from the $R(\theta)$ data in (b) and the lines from the $R(H)$ data in $H||c$ and $H||ab$ directions, respectively.

MR of a CDW was previously observed in 2H-$NbSe_2$ single crystal and interpreted as the magnetic breakdown through CDW gaps in the CDW state.[44] Interestingly, the MR observed in ultrathin 2H-$NbSe_2$ is much smaller than that in bulk samples.[44] A large MR is usually related to a high mobility.[45,46] For a thin film, extrinsic surface effects, for example surface oxidation,[21] usually cause a decrease in the mobility.[47] Nevertheless, we found that the amplitude of magnetoresistance in 2H-$NbSe_2$ shows a positive correlation to its *rrr* value even for bulk samples (data are not shown here). Since *rrr* is the resistivity ratio, which is independent of the surface factor, the suppression of MR cannot be due to surface oxidation in 2H-$NbSe_2$. Thus the suppression of MR may be due to enhanced electron correlation in the ultrathin sample. Such a conjecture is based on the facts that electron correlation usually decreases the electron mobility and the strength of electron correlation usually increases in low-dimensional system.

In Fig. 2(b), we show the angular (θ)-dependent magnetoresistance (ADMR) curves measured at 8 K and H ranging from 1 T to 9 T for ultrathin 2H-$NbSe_2$ film. Here, θ is the angle between the magnetic field H and the c crystalline direction of 2H-$NbSe_2$ as shown in the inset. In Fig. 2(c), we plot $R(\theta)$ at 8 K as a function of $\varepsilon_\theta = (\cos^2\theta + \gamma_{\mathrm{CDW}}^{-2}\sin^2\theta)^{1/2}$ for the ultrathin and bulk samples on the left and right axes, respectively. γ_{CDW} is the MR anisotropy, which can be obtained from the $R(\theta)$ curves or $R(H)$s with H along the ab and c directions. By tuning $R(\varepsilon_\theta H)$, curves (symbols) overlap at different H and θ and we found that $\gamma_{\mathrm{CDW}} \approx 8$ for ultrathin samples. We also investigated the data for $R(H_{||ab}/\gamma_{\mathrm{CDW}})$ (red lines) and $R(H_{||c})$ (black lines) in Fig. 2(c). We found that $\gamma_{\mathrm{CDW}} \approx 8$ and ≈ 6 for the ultrathin and bulk samples, respectively. The scaling behavior $R(\varepsilon_\theta H)$ was previously observed in the TMDC WTe_2,[48] where the ε_θ is attributed to the mass anisotropy $\gamma = (m_c^*/m_{ab}^*)^{1/2}$. 2H-$NbSe_2$ has a quasi-two-dimensional layered structure on which the pronounced 3D character of the electronic structure forms.[49] Thus 2H-$NbSe_2$ has multiple Fermi surface sheets of mixed dimensionality.[50] Previous experiments on plasma frequency showed the effective-mass anisotropy $\gamma = (m_c^*/m_{ab}^*)^{1/2}$ for 2H-$NbSe_2$ to be 2.24,[51] which is less than the γ_{CDW} obtained here. This suggests that the MR or CDW is related to the quasi-2D Fermi surface sheets in 2H-$NbSe_2$. Thus γ_{CDW} should not change a lot with the thickness of 2H-$NbSe_2$, which is consistent with the results that $\gamma_{\mathrm{CDW}} \approx 8$ and ≈ 6 for ultrathin and bulk samples, respectively.

4. Conclusion

In summary, detailed magnetotransport measurements were performed on 2H-$NbSe_2$ samples. In the CDW state, the ADMR obeys the scaling behavior $H(\cos^2\theta + \gamma_{\mathrm{CDW}}^{-2}\sin^2\theta)^{1/2}$. The CDW anionotropies (γ_{CDW}) are much larger than the effective mass anisotropy and do not change a lot as the sample thickness is reduced. The superconducting anisotropy increases significantly with decreasing sample thickness. Our results suggest three-dimensional superconductivity and a quasi-two dimensional feature of CDW in bulk 2H-$NbSe_2$.

Acknowledgments

Project supported by the National Natural Science Foundation of China (Grant Nos. 11574338 and 12074038) and NSAF (Grant No. U1530402).

References

[1] Grüner G 1988 *Rev. Mod. Phys.* **60** 1129
[2] Zaanen J and Gunnarsson O 1989 *Phys. Rev. B* **40** 7391
[3] Tranquada J, Sternlieb B, Axe J, Nakamura Y and Uchida S 1995 *Nature* **375** 561
[4] Wise W, Boyer M, Chatterjee K, Kondo T, Takeuchi T, Ikuta H, Wang Y and Hudson E 2008 *Nat. Phys.* **4** 696

[5] Chang J, Blackburn E, Holmes A, Christensen N B, Larsen J, Mesot J, Liang R, Bonn D, Hardy W, Watenphul A, *et al.* 2012 *Nat. Phys.* **8** 871
[6] Achkar A, Sutarto R, Mao X, He F, Frano A, Blanco-Canosa S, Le Tacon M, Ghiringhelli G, Braicovich L, Minola M, *et al.* 2012 *Phys. Rev. Lett.* **109** 167001
[7] Comin R, Frano A, Yee M M, Yoshida Y, Eisaki H, Schierle E, Weschke E, Sutarto R, He F, Soumyanarayanan A, *et al.* 2014 *Science* **343** 390
[8] da Silva Neto E H, Aynajian P, Frano A, Comin R, Schierle E, Weschke E, Gyenis A, Wen J, Schneeloch J, Xu Z, *et al.* 2014 *Science* **343** 393
[9] Xi X, Zhao L, Wang Z, Berger H, Forró L, Shan J and Mak K F 2015 *Nat. Nanotechnol.* **10** 765
[10] Ugeda M M, Bradley A J, Zhang Y, Onishi S, Chen Y, Ruan W, Ojeda-Aristizabal C, Ryu H, Edmonds M T, Tsai H Z, Riss A, Mo S K, Lee D, Zettl A, Hussain Z, Shen Z X and Crommie M F 2016 *Nat. Phys.* **12** 92
[11] Wilson J A, Di Salvo F and Mahajan S 1975 *Adv. Phys.* **24** 117
[12] Moncton D E, Axe J D and DiSalvo F J 1977 *Phys. Rev. B* **16** 801
[13] Moncton D, Axe J and DiSalvo F 1975 *Phys. Rev. Lett.* **34** 734
[14] Berthier C, Molinié P and Jérome D 1976 *Solid State Commun.* **18** 1393
[15] Cho K, Kończykowski M, Teknowijoyo S, Tanatar M A, Guss J, Gartin P, Wilde J M, Kreyssig A, McQueeney R, Goldman A I, *et al.* 2018 *Nat. Commun.* **9** 1
[16] Wang H, Huang X, Lin J, Cui J, Chen Y, Zhu C, Liu F, Zeng Q, Zhou J, Yu P, *et al.* 2017 *Nat. Commun.* **8** 1
[17] Xing Y, Zhao K, Shan P, Zheng F, Zhang Y, Fu H, Liu Y, Tian M, Xi C, Liu H, Feng J, Lin X, Ji S, Chen X, Xue Q K and Wang J 2017 *Nano Lett.* **17** 6802
[18] Noat Y, Silva-Guillén J A, Cren T, Cherkez V, Brun C, Pons S, Debontridder F, Roditchev D, Sacks W, Cario L, Ordejón P, García A and Canadell E 2015 *Phys. Rev. B* **92** 134510
[19] Khestanova E, Birkbeck J, Zhu M, Cao Y, Yu G L, Ghazaryan D, Yin J, Berger H, Forró L, Taniguchi T, Watanabe K, Gorbachev R V, Mishchenko A, Geim A K and Grigorieva I V 2018 *Nano Lett.* **18** 2623
[20] Staley N E, Wu J, Eklund P, Liu Y, Li L and Xu Z 2009 *Phys. Rev. B* **80** 184505
[21] Cao Y, Mishchenko A, Yu G, Khestanova E, Rooney A, Prestat E, Kretinin A, Blake P, Shalom M B, Woods C, *et al.* 2015 *Nano Lett.* **15** 4914
[22] Xi X, Wang Z, Zhao W, Park J H, Law K T, Berger H, Forró L, Shan J and Mak K F 2016 *Nat. Phys.* **12** 139
[23] Soumyanarayanan A, Yee M M, He Y, Van Wezel J, Rahn D J, Rossnagel K, Hudson E, Norman M R and Hoffman J E 2013 *Proc. Natl. Acad. Sci. USA* **110** 1623
[24] Wang C, Giambattista B, Slough C, Coleman R and Subramanian M 1990 *Phys. Rev. B* **42** 8890
[25] Hess H, Robinson R and Waszczak J 1991 *Physics B* **169** 422
[26] Ramos S L L M, Plumadore R, Boddison-Chouinard J, Hla S W, Guest J R, Gosztola D J, Pimenta M A and Luican-Mayer A 2019 *Phys. Rev. B* **100** 165414
[27] Coelho P M, Lasek K, Nguyen Cong K, Li J, Niu W, Liu W, Oleynik I I and Batzill M 2019 *J. Phys. Chem. Lett.* **10** 4987
[28] Nakata Y, Sugawara K, Chainani A, Oka H, Bao C, Zhou S, Chuang P Y, Cheng C M, Kawakami T, Saruta Y, *et al.* 2021 *Nat. Commun.* **12** 5873
[29] Ong N 1982 *Can. J. Phys.* **60** 757
[30] Grüner G 1988 *Rev. Mod. Phys.* **60** 1129
[31] Naito M and Tanaka S 1982 *J. Phys. Soc. Jpn.* **51** 219
[32] Jin Z, Li X, Mullen J T and Kim K W 2014 *Phys. Rev. B* **90** 045422
[33] Lei L, Zhang C, Yu A, Wu Y, Peng W, Xiao H, Qiao S and Hu T 2021 *Supercond. Sci. Technol.* **34** 025019
[34] Sinchenko A A, Grigoriev P D, Lejay P and Monceau P 2017 *Phys. Rev. B* **96** 245129
[35] Feng Y, Wang Y, Silevitch D, Yan J Q, Kobayashi R, Hedo M, Nakama T, Ōnuki Y, Suslov A, Mihaila B, *et al.* 2019 *Proc. Natl. Acad. Sci. USA* **116** 11201
[36] Inagaki K, Matsuura T, Tsubota M, Uji S, Honma T and Tanda S 2016 *Phys. Rev. B* **93** 075423
[37] Zhao Y, Liu H, Yan J, An W, Liu J, Zhang X, Wang H, Liu Y, Jiang H, Li Q, Wang Y, Li X Z, Mandrus D, Xie X C, Pan M and Wang J 2015 *Phys. Rev. B* **92** 041104
[38] He J, Wen L, Wu Y, Liu J, Tang G, Yang Y, Xing H, Mao Z, Sun H and Liu Y 2018 *Appl. Phys. Lett.* **113** 192401
[39] Zhang C, Hu T, Wang T, Wu Y, Yu A, Chu J, Zhang H, Zhang X, Xiao H, Peng W, Di Z, Qiao S and Mu G 2021 *2D Mater.* **8** 025024
[40] Li L J, Xu Z A, Shen J Q, Qiu L M and Gan Z H 2005 *J. Phys.: Condens. Matter* **17** 493
[41] Benyamini A, Telford E, Kennes D, Wang D, Williams A, Watanabe K, Taniguchi T, Shahar D, Hone J, Dean C, *et al.* 2019 *Nat. Phys.* **15** 947
[42] Ephron D, Yazdani A, Kapitulnik A and Beasley M 1996 *Phys. Rev. Lett.* **76** 1529
[43] Geshkenbein V, Larkin A, Feigel'Man M and Vinokur V 1989 *Physica C* **162–164** 239
[44] Naito M and Tanaka S 1982 *J. Phys. Soc. Jpn.* **51** 228
[45] Liang T, Gibson Q, Ali M N, Liu M, Cava R and Ong N 2015 *Nat. Mater.* **14** 280
[46] Shekhar C, Nayak A K, Sun Y, Schmidt M, Nicklas M, Leermakers I, Zeitler U, Skourski Y, Wosnitza J, Liu Z, *et al.* 2015 *Nat. Phys.* **11** 645
[47] Woods J M, Shen J, Kumaravadivel P, Pang Y, Xie Y, Pan G A, Li M, Altman E I, Lu L and Cha J J 2017 *ACS Appl. Mater. & Inter.* **9** 23175
[48] Thoutam L, Wang Y, Xiao Z, Das S, Luican-Mayer A, Divan R, Crabtree G and Kwok W 2015 *Phys. Rev. Lett.* **115** 046602
[49] Weber F, Hott R, Heid R, Lev L L, Caputo M, Schmitt T and Strocov V N 2018 *Phys. Rev. B* **97** 235122
[50] Johannes M D, Mazin I I and Howells C A 2006 *Phys. Rev. B* **73** 205102
[51] Dordevic S, Basov D, Dynes R and Bucher E 2001 *Phys. Rev. B* **64** 161103